
DYNAMIC LEARNING RATE FOR DEEP REINFORCEMENT LEARNING: A BANDIT APPROACH

PREPRINT

Henrique Donâncio¹, Antoine Barrier², Leah F. South³, and Florence Forbes¹

¹Univ. Grenoble Alpes, Inria, CNRS, Grenoble, France

²Univ. Grenoble Alpes, Inserm, U1216, Grenoble Institut Neurosciences, GIN, Grenoble, France

³School of Mathematical Sciences and Centre for Data Science, Queensland University of
Technology, Brisbane, Australia

February 4, 2025

ABSTRACT

In deep Reinforcement Learning (RL) models trained using gradient-based techniques, the choice of optimizer and its learning rate are crucial to achieving good performance: higher learning rates can prevent the model from learning effectively, while lower ones might slow convergence. Additionally, due to the non-stationarity of the objective function, the best-performing learning rate can change over the training steps. To adapt the learning rate, a standard technique consists of using decay schedulers. However, these schedulers assume that the model is progressively approaching convergence, which may not always be true, leading to delayed or premature adjustments. In this work, we propose dynamic Learning Rate for deep Reinforcement Learning (LRRL), a meta-learning approach that selects the learning rate based on the agent’s performance during training. LRRL is based on a multi-armed bandit algorithm, where each arm represents a different learning rate, and the bandit feedback is provided by the cumulative returns of the RL policy to update the arms’ probability distribution. Our empirical results demonstrate that LRRL can substantially improve the performance of deep RL algorithms for some tasks.

1 Introduction

Reinforcement Learning (RL), when combined with function approximators such as Artificial Neural Networks (ANNs), has shown success in learning policies that outperform humans in complex games by leveraging extensive datasets (see, *e.g.*, 37, 20, 43, 44). While ANNs were previously used as value function approximators [32], the introduction of Deep Q-Networks (DQN) by Mnih et al. [25, 26] marked a significant breakthrough by improving learning stability through two mechanisms: the target network and experience replay.

Experience replay (see 23) stores the agent’s interactions within the environment, allowing sampling of past interactions in a random way that disrupts their correlation. The target network further stabilizes the learning process by periodically copying the parameters of the learning network. This strategy is necessary because the Bellman update—using estimations to update other estimations—would otherwise occur using the same network, potentially causing divergence. By leveraging the target network, gradient steps are directed towards a periodically fixed target, ensuring more stability in the learning process. Additionally, the learning rate¹ hyperparameter controls the magnitude of these gradient steps in optimizers such as the Stochastic Gradient Descent (SGD) algorithm, affecting the training convergence.

¹The terms “learning rate” and “step-size” are used interchangeably in the literature and they technically refer to the same concept.

The learning rate is one of the most important hyperparameters, with previous work demonstrating that decreasing its value during policy finetuning can enhance performance by up to 25% in vanilla DQN [3]. Determining the appropriate learning rate is essential for achieving good model performance: higher values can prevent the agent from learning, while lower values can lead to slow convergence (see 15, 7, 46). However, finding a learning rate value that improves the model performance requires extensive and computationally expensive testing. In order to adapt its initial choice during training, optimizers such as Adam [18] and RMSProp [41] employ an internal scheme that dynamically adjusts the learning rate, considering, for instance, past gradient information. Therefore, various learning rate scheduling strategies can be combined with the optimizer to decrease the learning rate and improve the convergence over the training steps.

Standard learning rate schedulers typically decrease the learning rate based on training progress using, *e.g.*, linear or exponential decay strategies [35, 46]. Unlike supervised learning, RL usually involves generating data by trading off between exploration (discovery of new states) and exploitation (refining of the agent’s knowledge). As the policy improves, the data distribution encountered by the agent becomes more concentrated, but this evolution occurs at a different pace than the overall training progress. For instance, some environments require extensive exploration due to the sparseness of rewards, while others need more exploitation to refine the policy to the complexity of the task. Consequently, a more sophisticated decaying learning rate strategy that accounts for policy performance rather than training steps can significantly enhance learning in deep RL.

Contributions. In this work, we propose dynamic **Learning Rate** for deep **Reinforcement Learning** (LRRL), a method to select the learning rate *on the fly* for deep RL. Our approach acknowledges that *different learning phases require different learning rates*, and as such, instead of scheduling the learning rate decay using some blanket approach, we dynamically choose the learning rate using a Multi-Armed Bandit (MAB) algorithm, which accounts for the current policy’s performance. Our method has the advantage of being algorithm-agnostic and applicable to any optimizer. By exploiting different configurations, we aim to illustrate the use cases of LRRL and assess its robustness. We provide experiments with the Adam and RMSProp optimizers, with different sets of arms, and two deep RL algorithms (DQN and IQN). Tests are carried out across a variety of Atari games, using baselines provided in the Dopamine framework (see 9). We also show the effectiveness of LRRL using a standard SGD optimizer in a non-RL optimization context. Related work is detailed in Appendix A. Our main contributions and results can be summarized as follows:

- We introduce LRRL, a novel approach that leverages a MAB algorithm to dynamically select the learning rate during training in deep RL.
- We assess LRRL robustness across a set of Atari games, using different configurations, optimizers and deep RL algorithms. Our empirical results demonstrate that LRRL achieves performance competitive with or superior to standard learning using fixed learning rates or decay schedulers. We further highlight its advantages by considering an SGD optimizer on stationary non-convex landscapes.
- More generally, we show that LRRL matches the scheduler’s behavior by dynamically choosing lower learning rate values as the training progresses.

2 Preliminaries

This section introduces the RL and MAB frameworks, defining supporting notation.

2.1 Deep Reinforcement Learning

An RL task is defined by a Markov Decision Process (MDP), that is by a tuple $(\mathcal{S}, \mathcal{A}, P, R, \gamma, T)$, where \mathcal{S} denotes the state space, \mathcal{A} the set of possible actions, $P : \mathcal{S} \times \mathcal{A} \times \mathcal{S} \rightarrow [0, 1]$ the transition probability, $R : \mathcal{S} \times \mathcal{A} \rightarrow \mathbb{R}$ the reward function, $\gamma \in [0, 1]$ the discount factor, and T the horizon length in episodic settings (see, *e.g.*, 39 for details). In RL, starting from an initial state s_0 , a learner called the *agent* interacts with the environment by picking, at time t , an action a_t depending on the current state s_t . In return, it receives a reward $r_t = R(s_t, a_t)$, reaching a new state s_{t+1} according to the transition probability $P(\cdot | s_t, a_t)$. The agent’s objective is to learn a policy $\pi(\cdot | s)$ that maps a state s to a probability distribution over actions in \mathcal{A} , aiming to maximize expected returns $Q^\pi(s, a) = \mathbb{E}_\pi \left[\sum_{t=0}^T \gamma^t r_t \mid s_0 = s, a_0 = a \right]$.

To learn how to perform a task, value function-based algorithms coupled with ANNs [25, 26] approximate the *quality* of a given state-action pair $Q(s, a)$ using parameters θ to derive a policy $\pi_\theta(\cdot | s) = 1_{a^*(s)}(\cdot)$ where $1_{a^*(s)}$ denotes the uniform distribution over $a^*(s)$ with $a^*(s) = \arg \max_{a \in \mathcal{A}} Q_\theta(s, a)$. By storing transitions $(s, a, r, s') =$

(s_t, a_t, r_t, s_{t+1}) into the replay memory \mathcal{D} , the objective is to minimize the loss function defined by:

$$\mathcal{J}(\theta) = \mathbb{E}_{(s,a,r,s') \sim \mathcal{D}} \left[r + \gamma \max_{a' \in \mathcal{A}} Q_{\theta^-}(s', a') - Q_{\theta}(s, a) \right]^2, \quad (1)$$

where θ^- are the target network parameters used to compute the target of the learning network $y = r + \gamma \max_{a' \in \mathcal{A}} Q_{\theta^-}(s', a')$. The parameters θ^- are periodically updated by copying the parameters θ , leveraging stability during the learning process by fixing the target y . The minimization, and hence the update of the parameters θ , is done according to the optimizer's routine. A simple possibility is to use SGD using mini-batch approximations of the loss gradient:

$$\begin{aligned} \theta_{n+1} &\leftarrow \theta_n - \eta \nabla_{\theta} \mathcal{J}(\theta_n), \text{ where} \\ \nabla_{\theta} \mathcal{J}(\theta_n) &\approx \frac{1}{|\mathcal{B}|} \sum_{(s,a,r,s') \in \mathcal{B}} 2(Q_{\theta}(s, a) - y) \nabla_{\theta} Q_{\theta}(s, a), \end{aligned} \quad (2)$$

with \mathcal{B} being a mini-batch of transitions sampled from \mathcal{D} and η is a single scalar value called the *learning rate*. Unlike in supervised learning, where the loss function $\mathcal{J}(\theta)$ is typically stationary, RL presents a fundamentally different challenge: the policy is continuously evolving, leading to shifting distributions of states, actions, and rewards over time. This continuous evolution introduces instability during learning, which deep RL mitigates by employing a large replay memory and calculating the target using a *frozen* network with parameters θ^- . However, stability also depends on how the parameters θ change during each update. This work aims to adapt to these changes by dynamically selecting the learning rate η over the training steps.

2.2 Multi-Armed Bandits

MAB provide an elegant framework for making sequential decisions under uncertainty (see for instance 21). MAB can be viewed as a special case of RL with a single state, where at each round n , the agent selects an arm $k_n \in \{1, \dots, K\}$ from a set of K arms and receives a feedback (reward) $f_n(k_n) \in \mathbb{R}$. Like RL, MAB algorithms must balance the trade-off between exploring arms that have been tried less frequently and exploiting arms that have yielded higher rewards up to time n .

To account for the non-stationarity of RL rewards, we will consider in this work the MAB setting of adversarial bandits [6]. In this setting, at each round n , the agent selects an arm k_n according to some distribution p_n while the environment (the *adversary*) arbitrarily (e.g., without stationary constraints) determines the rewards $f_n(k)$ for all arms $k \in \mathcal{K}$. MAB algorithms are designed to minimize the *pseudo-regret* G_N after N rounds defined by:

$$G_N = \mathbb{E} \left[\sum_{n=1}^N \max_{k \in \{1, \dots, K\}} f_n(k) - \sum_{n=1}^N f_n(k_n) \right],$$

where the randomness of the expectation depends on the MAB algorithm and on the adversarial environment, $\sum_{n=1}^N \max_{k \in \{1, \dots, K\}} f_n(k)$ represents the accumulated reward of the (potentially changing) single best arm, and $\sum_{n=1}^N f_n(k_n)$ is the accumulated reward obtained by the algorithm. A significant component in the adversarial setting is to ensure that each arm k has a non-zero probability $p_n(k) > 0$ of being selected at each round n : this guarantees exploration, which is essential for the algorithm's robustness to environment changes.

3 Dynamic Learning Rate for Deep RL

In this section, we tackle the challenge of selecting the learning rate over the training steps by introducing a dynamic LRRL. LRRL is a meta-learning approach designed to dynamically select the learning rate in response to the agent's performance. LRRL couples with SGD optimizers and adapts the learning rate based on the reward achieved by the policy π_{θ} using an adversarial MAB algorithm. As the agent interacts with the environment, the average of observed rewards is used as bandit feedback to guide the selection of the most appropriate learning rate throughout the training process.

3.1 Selecting the Learning Rate Dynamically

Our problem can be framed as selecting a learning rate η for policy updates —specifically, when updating the parameters θ after λ interactions with the environment.

Before training, a set $\mathcal{K} = \{\eta_1, \dots, \eta_K\}$ of K learning rates are defined by the user. Then, during training, a MAB algorithm selects, at every round n —that is, at every κ interactions with the environment—an arm $k_n \in \{1, \dots, K\}$

according to a probability distribution p_n defined based on previous rewards, as explained in the next section. The parameters θ are then updated using the sampled learning rate η_{k_n} . The steps involved in this meta-learning approach are summarized in Algorithm 1.

Algorithm 1 dynamic Learning Rate for deep Reinforcement Learning (LRRL)

Parameters:

Set of learning rates $\mathcal{K} = \{\eta_1, \dots, \eta_K\}$
 Number of episodes M
 Horizon length T
 Update window λ for the learning network θ
 Update window τ for the target network θ^-
 Update window κ for arm probabilities p

Initialize:

Parameters θ and θ^-
 Arm probabilities $p_0 \leftarrow (\frac{1}{K}, \dots, \frac{1}{K})$
 MAB round $n \leftarrow 0$
 Cumulative reward $R \leftarrow 0$
 Environment interactions counter $C \leftarrow 0$

for episode $m = 1, 2, 3, \dots, M$ **do**

for timestep $t = 1, 2, 3, \dots, T$ **do**

 Choose action a_t following the policy $\pi_\theta(s)$ with probability $1 - \epsilon$ $\triangleright (\epsilon$ -greedy strategy)

 Play action a_t and observe reward r_t

 Add r_t to cumulative reward $R \leftarrow R + r_t$

 Increase environment interactions counter $C \leftarrow C + 1$

if $C \bmod \lambda \equiv 0$ **then**

if $C \geq \kappa$ **then**

 Compute average of the last C rewards $f_n \leftarrow \frac{R}{C}$

 Increase MAB round $n \leftarrow n + 1$

 Compute weights w_n and arm probabilities p_n using Equations (3, 4)

 Sample arm k_n with distribution p_n

 Reset $R \leftarrow 0$ and $C \leftarrow 0$

end if

 Update network parameter θ using the optimizer update rule with learning rate η_{k_n}

 Every τ steps update the target network $\theta^- \leftarrow \theta$

end if

end for

end for

Note that the same algorithm might be used with learning rates schedulers, that is with $\mathcal{K} = \{\eta_1, \dots, \eta_K\}$ where $\eta_k : \mathbb{N} \rightarrow \mathbb{R}_+$ is a predefined function, usually converging towards 0 at infinity. If so, the learning rate used at round n of the optimization is $\eta_{k_n}(n)$.

3.2 Updating the Probability Distribution

As we expect that the agent’s performance—and hence, the cumulative rewards—will improve over time, the MAB algorithm should receive non-stationary feedback. To take this non-stationary nature of the learning into account, we employ a modified version of the Exponential-weight algorithm for Exploration and Exploitation (Exp3, see 6 for an introduction). At round n , Exp3 chooses the next arm (and its associated learning rate) according to the arm probability distribution p_n which is based on weights $(w_n(k))_{1 \leq k \leq K}$ updated recursively. Those weights incorporate a time-decay factor $\delta \in (0, 1]$ that increases the importance of recent feedback, allowing the algorithm to respond more quickly to changes of the best action and to improvements in policy performance.

Specifically, after picking arm k_n at round n , the RL agent interacts C times with the environment and the MAB algorithm receives a feedback f_n corresponding to the average reward of those C interactions. Based on Moskovitz et al. [27], this feedback is then used to compute the *improvement in performance*, denoted by f'_n , obtained by subtracting the average of the past j bandit feedbacks from the most recent one f_n :

$$f'_n = f_n - \frac{1}{j} \sum_{i=0}^{j-1} f_{n-i}.$$

The improvement in performance allows computation of the next weights w_{n+1} as follows, where initially $w_1 = (0, \dots, 0)$:

$$\forall k \in \{1, \dots, K\}, \quad w_{n+1}(k) = \begin{cases} \delta w_n(k) + \alpha \frac{f'_n}{e^{w_n(k)}} & \text{if } k = k_n \\ \delta w_n(k) & \text{otherwise,} \end{cases} \quad (3)$$

where $\alpha > 0$ is a step-size parameter. The distribution p_{n+1} , used to draw the next arm k_{n+1} , is

$$\forall k \in \{1, \dots, K\}, \quad p_{n+1}(k) = \frac{e^{w_{n+1}(k)}}{\sum_{k'=1}^K e^{w_{n+1}(k')}}. \quad (4)$$

This update rule ensures that as the policy π_θ improves the cumulative reward, the MAB algorithm continues to favor learning rates that are most beneficial under the current policy performance, thereby effectively handling the non-stationarity inherent in the learning process.

4 Experiments

In the following sections, we examine whether combining LRRL with Adam or RMSProp —two widely used optimization algorithms— can enhance cumulative returns in deep RL algorithms. We compare LRRL against learning methods both with and without schedulers, using baseline algorithms provided in the Dopamine [9] framework. The experiments involve testing LRRL across various configurations and a selection of Atari games, reporting the mean and one-half standard deviation of returns over 5 independent runs. As testing the full Atari benchmark is extremely costly, we choose a representative subset of games guided by their baseline learning curves, which offer insights into reward sparsity, stochasticity, and exploration demands. Further details on the evaluation metrics and hyperparameters used in these experiments are provided in Appendices C and D. In addition, although our primary target is RL tasks, we also test LRRL using SGD to minimize stationary objective functions to provide a simpler evaluation, as performance in RL is highly multi-factorial.

4.1 Comparing LRRL with Standard Learning

In our first experiment, we consider a set of 5 learning rates. We set different configurations of LRRL using these values and compare them against the DQN agent reaching the best performance, in terms of maximum average return, among the possible single rates. More specifically, the learning rates considered are

$$\mathcal{K}(5) = \{1.5625 \times 10^{-5}, 3.125 \times 10^{-5}, 6.25 \times 10^{-5}, 1.25 \times 10^{-4}, 2.5 \times 10^{-4}\}.$$

The whole set $\mathcal{K}(5)$ of rates is used by one LRRL version, while others are based on the 3 lowest ($\mathcal{K}_{\text{lowest}}(3)$), 3 middle ($\mathcal{K}_{\text{middle}}(3)$), 3 highest ($\mathcal{K}_{\text{highest}}(3)$) values, and the last one ($\mathcal{K}_{\text{sparse}}(3)$) taking the lowest/middle/highest values. All experiments use the Adam optimizer, and we report the return based on the same number of environment iterations. The results in Figure 1 demonstrate that LRRL using the full set $\mathcal{K}(5)$ substantially outperforms the best-performing single learning rate in 2 out of 6 games (Seaquest and Breakout) while remaining competitive in the others. As shown in Figure 7 in Appendix B.1, the baseline DQN performance is highly sensitive to the learning rate choice, requiring extensive hyperparameter tuning to identify the optimal rate. In contrast, LRRL dynamically selects learning rates during training, avoiding the need for such tuning. Additionally, the 3-arm bandit variants highlight that while LRRL can explore multiple learning rates within a single run, the specific set of rates available still impacts performance. Overall, these results illustrate the advantage of LRRL, which achieves similar or better performance than the best-tuned DQN baseline while eliminating the computational cost of manual learning rate tuning.

Next, we illustrate how LRRL adapts during training in response to non-stationary bandit feedback as policy performance improves. Figure 2 shows the systematic sampling of pulled arms (learning rates) and corresponding returns over training steps from a single run of LRRL $\mathcal{K}(5)$. In most of the tested environments, LRRL behaves similarly to time-decay schedulers by selecting higher learning rates during the early stages of training, gradually shifting toward arms with lower rates as training progresses.

4.2 Combining and Comparing Schedulers with LRRL

In the following experiments, LRRL is combined with learning rate schedulers. Specifically, we employ schedulers with exponential decay rate of the form $\eta(n) = \eta_0 \times e^{-d n}$, where η_0 is a fixed initial value (common to each scheduler and equal to 6.25×10^{-5} in our experiment), d is the exponential decay rate and n is the number of policy updates (*i.e.*, of MAB rounds). We define a set of 3 schedulers \mathcal{K}_s , where each arm represents a scheduler using a different

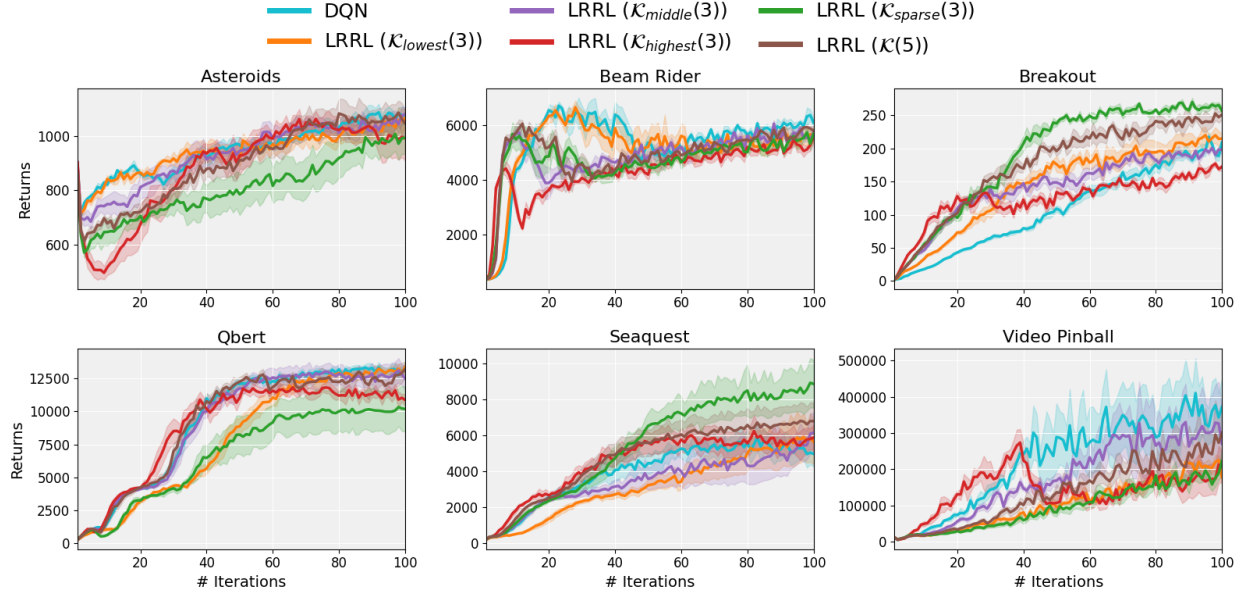


Figure 1: Comparison between LRRL and standard DQN learning: 5 variants of LRRL with different learning rate sets (provided in Appendix D) are tested against the DQN algorithm reaching best performance among the possible learning rates. The mean and one-half standard deviations over 5 runs are respectively represented by the curves and shaded areas.

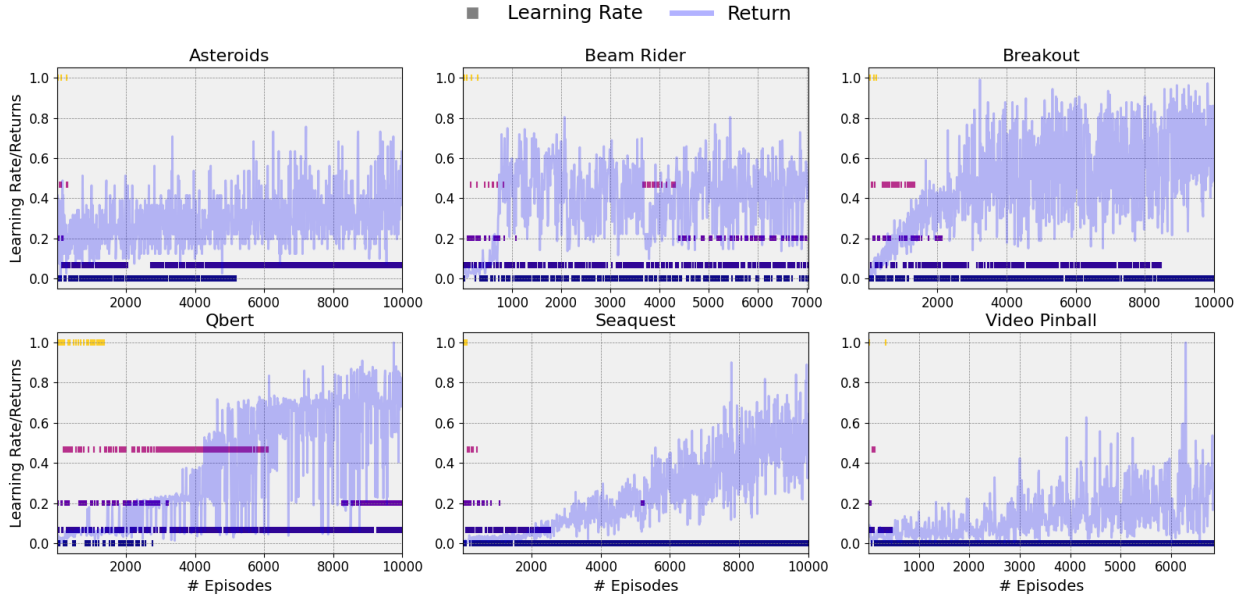


Figure 2: Systematic sampling of normalized learning rates and returns over the training steps using LRRL $\mathcal{K}(5)$ with Adam optimizer, through a single run. For each episode, we show the selected learning rate using different colors. Lower rates are increasingly selected over time.

decay rate $d = \{1, 2, 3\} \times 10^{-7}$, and compare the results of LRRL with each scheduler individually, using the Adam optimizer.

Figure 3 shows that LRRL combined with schedulers could once again substantially increase the final performance of 2 out of 6 tasks compared to using a fixed scheduler. In the remaining tasks, LRRL remains at least competitive, while for most of them, it shows a better jumpstart performance. The dashed black line represents the maximal average return achieved by Adam without learning rate decay, resulting in slightly worse performance compared to using schedulers, aligning with findings in previous work by Andrychowicz et al. [4], who linearly decay the learning rate to 0.

In all the experiments conducted so far, we have set the update window κ parameter to 1, which allows the observation of a full episode before updating the learning rate. In Appendix B.3, we address how this value could influence the performance of LRRL by allowing the observation of more interactions.

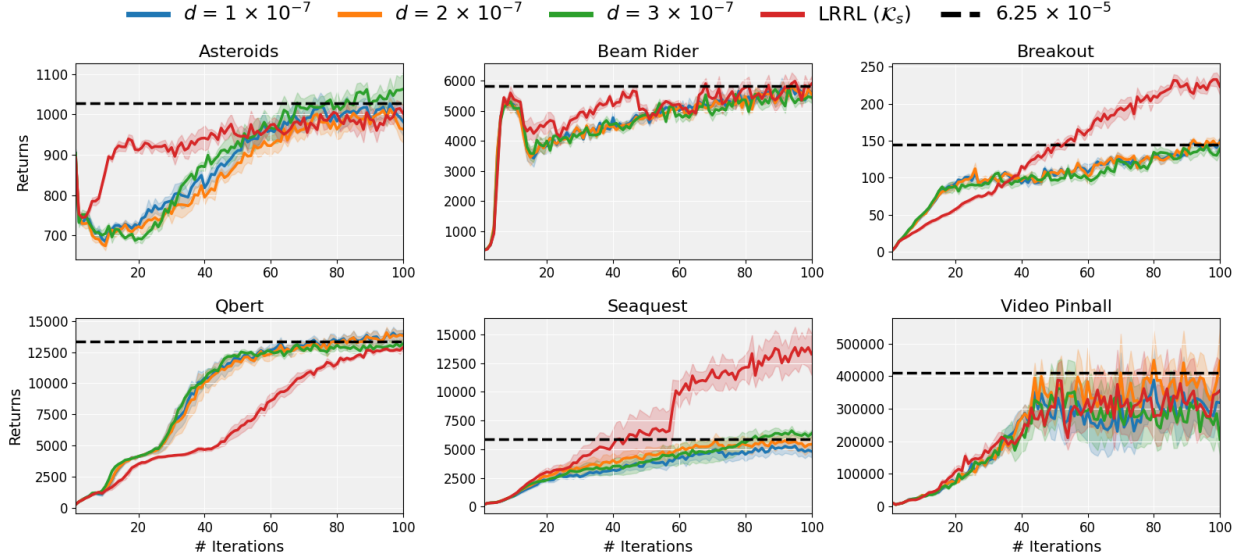


Figure 3: LRRL with arms that select learning rate schedulers: LRRL vs 3 individual schedulers ($d = 1, 2, 3$). The dashed black line represents the max average return achieved by Adam with a constant learning rate set to 6.25×10^{-5} .

4.3 Comparing RMSProp and Adam Optimizers

Another widely used optimizer for deep RL models is RMSProp, which, like Adam, features an adaptive learning rate mechanism. Adam builds upon RMSProp by retaining exponential moving averages to give more weight to recent gradients while incorporating momentum. Although the standard RMSProp does not feature momentum, we found that adding momentum to RMSProp can increase both the performance of DQN and LRRL, aligning with findings in the literature [30, 4]. In the following experiment, we compare the performance of RMSProp with Nesterov’s momentum (RMSProp-M), and Adam when coupled with either LRRL or the best-performing single learning rate when using DQN. Since the results were consistent in previous sections, we extend the experiments to other 3 Atari games.

Figure 4 shows that LRRL coupled with Adam consistently outperforms our configuration using RMSProp-M and the baseline using standard DQN. Moreover, LRRL (RMSProp-M) underperforms compared to DQN without LRRL in two out of three tasks due to its slow convergence despite better jumpstart performance. Future work should investigate whether this slow convergence is due to some optimizer features such as the absence of bias correction in the first and second moment estimates.

4.4 LRRL with a Distributional RL Algorithm

Lastly, we illustrate the versatility of LRRL by combining it with the distributional RL algorithm Implicit Quantile Networks (IQN) [11], which exhibits the best performance in many Atari games among the algorithms available in Dopamine. Adam is used as the optimizer. Figure 5 shows that LRRL outperforms standard learning with a single

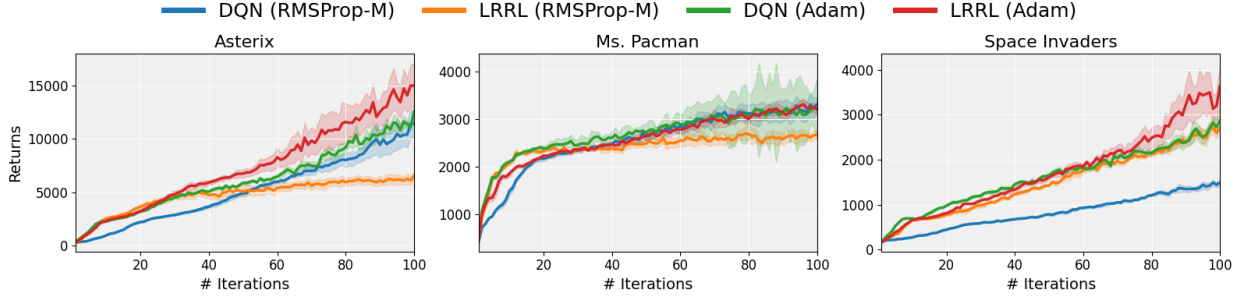


Figure 4: A comparison between Adam and RMSProp with momentum, using either DQN or LRRL.

learning rate across all the tasks evaluated. More generally, LRRL can be seamlessly integrated with *any* RL algorithm that employs function approximators based on SGD, improving its performance and mitigating hyperparameter tuning.

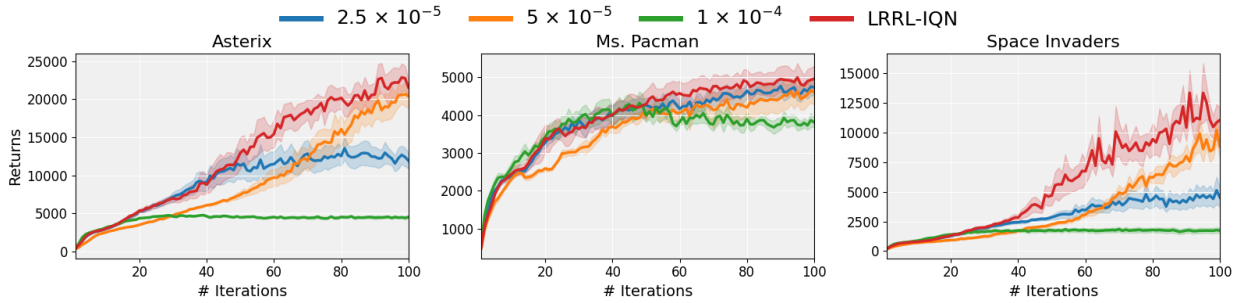


Figure 5: Comparison between LRRL and standard IQN learning: IQN combined with LRRL using 3 different learning rates is tested against the 3 variants of standard IQN using each possible learning rate.

4.5 SGD and Stationary Non-convex Loss Landscapes

Although RL tasks are a challenging showcase to illustrate the effectiveness of our approach in the non-stationary case, there are many confounding factors to analyze their impact on the results, such as the optimizer adaptive routine, the environment stochasticity, and the reward sparseness. To disentangle these factors from our evaluation, in the following experiments we employ the SGD optimizer, which has a single scalar learning rate without adaptive scheme or momentum to find the global minima of 6 non-convex loss landscapes. Since these functions represent a stationary case, we employ the stochastic bandit Minimax Optimal Strategy in the Stochastic case (MOSS) algorithm (see details in Appendix B.2), using as feedback the loss plus a small constant ξ , such that $f_n = \frac{1}{|\text{loss}(n)| + \xi}$, observed at each gradient step n to update the arm’s probabilities.

Figure 6 illustrates the performance of LRRL against SGD with a single learning rate, starting from the same initial point and for the same amount of steps. The final steps are indicated by a star icon with a different color. The results show that LRRL, with its “all-in-one” strategy, efficiently navigates intricate landscapes. It is effective in combining higher learning rates to accelerate convergence and lower ones for more fine-grained optimization steps when needed, as evidenced in the loss landscapes depicted in Figures 6a, 6b, and 6c. In addition, Figures 6d, 6e, and 6f illustrate that LRRL can be also effective in converging towards the best-performing learning rate within the arms, showcased by its steady convergence towards the global minima.

5 Conclusion

In this work, we introduced LRRL, a meta-learning approach for selecting optimizers’ learning rates on the fly. In any optimization task, the best-performing learning rate or rate scheduler is typically unknown, requiring multiple runs to test each candidate in a wasteful computational effort. LRRL mitigates this cost by employing a multi-armed bandit algorithm to explore a set of learning rates within a single run, significantly reducing the need for extensive hyperparameter tuning while achieving better or competitive results with minimal computational overhead. Using

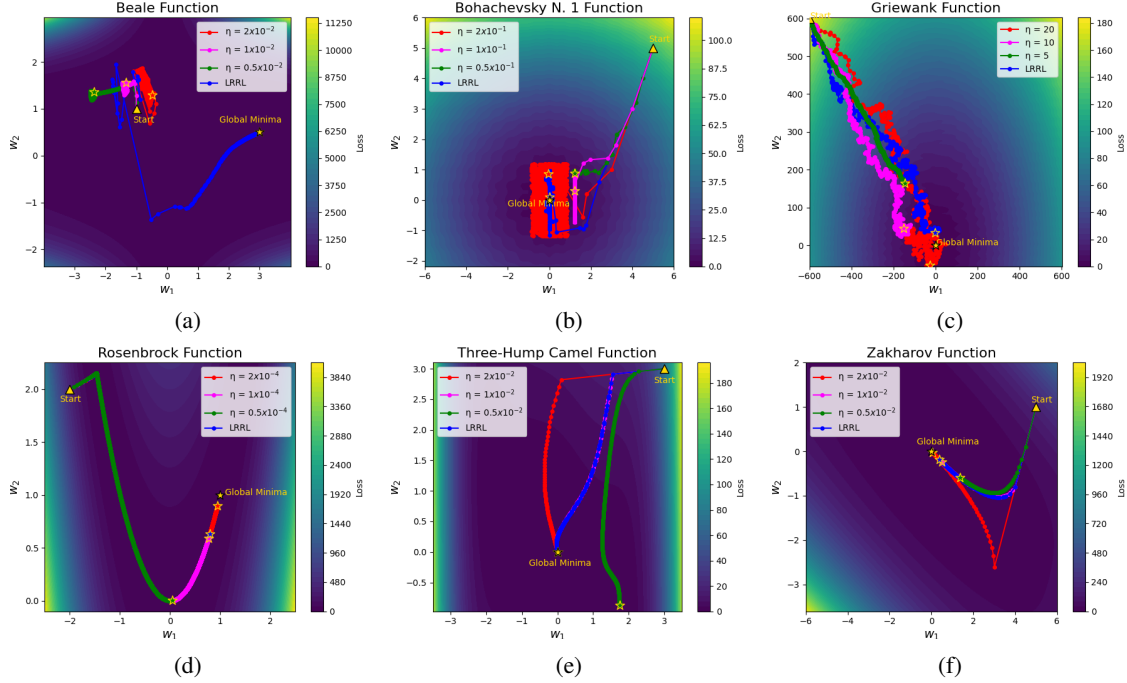


Figure 6: Comparison between LRRL and fixed learning rates in a stationary setting with SGD. LRRL with 3 learning rates is tested against the 3 constant rates for 6 non-convex losses (shown in Figure 10 in Appendix B.4). LRRL is effective in either converging to the best performing rate or combining the set to achieve better results.

RL and non-convex optimization tasks, our empirical results show that combining LRRL with the Adam or SGD optimizers could enhance the performance, outperforming baselines and learning rate schedulers.

Future investigations could extend LRRL ideas to other hyperparameters, such as mini-batch size, which also plays a key role in convergence. Moreover, although LRRL selects rates based on policy performance, alternative feedback mechanisms could be explored, such as using gradient information to select block-wise (*e.g.*, per-layer) learning rates, extending these ideas to supervised learning and applying them to other non-stationary objective functions, including those encountered in Continual Learning [33, 19, 1].

Limitations. The primary limitation of LRRL lies in the need to define a set of arms for the MAB algorithm, as the choice of this set can directly influence the performance of the underlying learning algorithm. However, in computationally intensive settings such as RL tasks, LRRL offers a significant advantage: it enables the simultaneous evaluation of multiple learning rates within a single training run, eliminating the need to test each rate individually. By employing an “all-in-one” strategy, LRRL not only achieves competitive results while reducing the burden of hyperparameter optimization but also can outperform standard learning by combining multiple learning rates.

Broader Impact Statement

This work aims to contribute to the advancement of the field of Machine Learning. While we did not identify any direct negative social impacts associated with this research, we encourage future studies building on it to remain vigilant and critically evaluate potential ethical and societal implications.

Acknowledgment

This work was granted access to the HPC resources of IDRIS under the allocation 2024-A0171015651 made by GENCI. HD and FF acknowledge funding from Inria Project WOMBAT. LFS is supported by a Discovery Early Career Researcher Award from the Australian Research Council (DE240101190)

References

- [1] D. Abel, A. Barreto, B. Van Roy, D. Precup, H. P. van Hasselt, and S. Singh. A Definition of Continual Reinforcement Learning. In *Advances in Neural Information Processing Systems*, volume 36, pages 50377–50407. Curran Associates, Inc., 2023.
- [2] R. Agarwal, D. Schuurmans, and M. Norouzi. An Optimistic Perspective on Offline Reinforcement Learning. In *Proceedings of the 37th International Conference on Machine Learning (ICML 2017)*, volume 119, pages 104–114. PMLR, 2020.
- [3] R. Agarwal, M. Schwarzer, P. S. Castro, A. C. Courville, and M. Bellemare. Reincarnating reinforcement learning: Reusing prior computation to accelerate progress. In *Advances in Neural Information Processing Systems*, volume 35, pages 28955–28971. Curran Associates, Inc., 2022.
- [4] M. Andrychowicz, A. Raichuk, P. Stańczyk, M. Orsini, S. Girgin, R. Marinier, L. Hussenot, M. Geist, O. Pietquin, M. Michalski, et al. What Matters for On-Policy Deep Actor-Critic Methods? A Large-Scale Study. In *9th International Conference on Learning Representations, ICLR 2021*, 2021.
- [5] J. Audibert and S. Bubeck. Minimax Policies for Adversarial and Stochastic Bandits. In *Proceedings of the 22nd Conference on Learning Theory (COLT 2009)*. PMLR, 2009.
- [6] P. Auer, N. Cesa-Bianchi, Y. Freund, and R. E. Schapire. The Nonstochastic Multiarmed Bandit Problem. *SIAM Journal on Computing*, 32(1):48–77, 2002. doi: 10.1137/S0097539701398375.
- [7] L. Blier, P. Wolinski, and Y. Ollivier. Learning with random learning rates. In *Machine Learning and Knowledge Discovery in Databases: European Conference, ECML PKDD 2019*, pages 449–464. Springer, 2019.
- [8] J. Bradbury, R. Frostig, P. Hawkins, M. J. Johnson, C. Leary, D. Maclaurin, G. Necula, A. Paszke, J. VanderPlas, S. Wanderman-Milne, and Q. Zhang. JAX: composable transformations of Python+NumPy programs, 2018. URL <http://github.com/google/jax>. version 0.3.13.
- [9] P. S. Castro, S. Moitra, C. Gelada, S. Kumar, and M. G. Bellemare. Dopamine: A Research Framework for Deep Reinforcement Learning, 2018. Preprint, arXiv:1812.06110.
- [10] J. Coullon, L. South, and C. Nemeth. Efficient and generalizable tuning strategies for stochastic gradient MCMC. *Statistics and Computing*, 33(3), 2023. doi: 10.1007/s11222-023-10233-3.
- [11] W. Dabney, G. Ostrovski, D. Silver, and R. Munos. Implicit Quantile Networks for Distributional Reinforcement Learning. In *Proceedings of the 35th International Conference on Machine Learning (ICML 2018)*, pages 1104–1113. PMLR, 2018.
- [12] G. DeepMind. The DeepMind JAX Ecosystem, 2020. URL <http://github.com/google-deepmind>.
- [13] T. Degris, K. Javed, A. Sharifnassab, Y. Liu, and R. S. Sutton. Step-size optimization for continual learning, 2024. Preprint, arXiv:2401.17401.
- [14] S. Fujimoto, D. Meger, and D. Precup. Off-Policy Deep Reinforcement Learning without Exploration. In *Proceedings of the 36th International Conference on Machine Learning (ICML 2019)*, volume 97, pages 2052–2062. PMLR, 2019.
- [15] I. Goodfellow, Y. Bengio, and A. Courville. *Deep Learning*. MIT Press, 2016.
- [16] K. G. Jamieson and A. Talwalkar. Non-stochastic Best Arm Identification and Hyperparameter Optimization. In *Proceedings of the 19th International Conference on Artificial Intelligence and Statistics, AISTATS 2016*, volume 51, pages 240–248. JMLR, 2016.
- [17] Z. Karnin, T. Koren, and O. Somekh. Almost Optimal Exploration in Multi-Armed Bandits. In *Proceedings of the 30th International Conference on Machine Learning (ICML 2013)*, volume 28(3), pages 1238–1246. PMLR, 2013.
- [18] D. P. Kingma and J. Ba. Adam: A method for stochastic optimization. In *3rd International Conference on Learning Representations, ICLR 2015*, 2015.
- [19] J. Kirkpatrick, R. Pascanu, N. C. Rabinowitz, J. Veness, G. Desjardins, A. A. Rusu, K. Milan, J. Quan, T. Ramalho, A. Grabska-Barwinska, D. Hassabis, C. Clopath, D. Kumaran, and R. Hadsell. Overcoming catastrophic forgetting in neural networks. *CoRR*, 2016. arXiv:1612.00796.
- [20] G. Lample and D. S. Chaplot. Playing FPS Games with Deep Reinforcement Learning. In *Proceedings of the AAAI Conference on Artificial Intelligence*, 2017.
- [21] T. Lattimore and C. Szepesvári. *Bandit Algorithms*. Cambridge University Press, 2020.

- [22] L. Li, K. G. Jamieson, G. DeSalvo, A. Rostamizadeh, and A. Talwalkar. Hyperband: a novel bandit-based approach to hyperparameter optimization. *Journal of Machine Learning Research*, 18(1):6765–6816, 2018. ISSN 1532-4435.
- [23] L. J. Lin. Self-Improving Reactive Agents Based On Reinforcement Learning, Planning and Teaching. *Machine Learning*, 8:293–321, 1992.
- [24] R. Liu, T. Wu, and B. Mozafari. Adam with Bandit Sampling for Deep Learning. In *Advances in Neural Information Processing Systems*, volume 33, pages 5393–5404. Curran Associates, Inc., 2020.
- [25] V. Mnih, K. Kavukcuoglu, D. Silver, A. Graves, I. Antonoglou, D. Wierstra, and M. A. Riedmiller. Playing Atari with Deep Reinforcement Learning. *CoRR*, 2013. arXiv:1312.5602.
- [26] V. Mnih, K. Kavukcuoglu, D. Silver, A. A. Rusu, J. Veness, M. G. Bellemare, A. Graves, M. Riedmiller, A. K. Fidjeland, G. Ostrovski, et al. Human-level control through deep reinforcement learning. *Nature*, 518(7540): 529–533, 2015.
- [27] T. Moskovitz, J. Parker-Holder, A. Pacchiano, M. Arbel, and M. Jordan. Tactical Optimism and Pessimism for Deep Reinforcement Learning. In *Advances in Neural Information Processing Systems*, volume 34, pages 12849–12863. Curran Associates, Inc., 2021.
- [28] G. Ostrovski, P. S. Castro, and W. Dabney. The Difficulty of Passive Learning in Deep Reinforcement Learning. In *Advances in Neural Information Processing Systems*, volume 34, pages 23283–23295, 2021.
- [29] J. Parker-Holder, V. Nguyen, and S. J. Roberts. Provably Efficient Online Hyperparameter Optimization with Population-Based Bandits. In *Advances in Neural Information Processing Systems*, volume 33, pages 17200–17211. Curran Associates, Inc., 2020.
- [30] N. Qian. On the momentum term in gradient descent learning algorithms. *Neural Networks*, 12(1):145–151, 1999. doi: 10.1016/S0893-6080(98)00116-6.
- [31] C. Rasmussen and C. Williams. *Gaussian Processes for Machine Learning*. Adaptive Computation and Machine Learning series. MIT Press, 2005. ISBN 9780262182539.
- [32] M. Riedmiller. Neural fitted q iteration – first experiences with a data efficient neural reinforcement learning method. In *Proceedings of the 16th European Conference on Machine Learning*, pages 317–328, Berlin, Heidelberg, 2005. Springer-Verlag. ISBN 3540292438. doi: 10.1007/11564096_32.
- [33] A. A. Rusu, N. C. Rabinowitz, G. Desjardins, H. Soyer, J. Kirkpatrick, K. Kavukcuoglu, R. Pascanu, and R. Hadsell. Progressive Neural Networks. *CoRR*, 2016. arXiv:1606.04671.
- [34] T. Schaul, J. Quan, I. Antonoglou, and D. Silver. Prioritized experience replay. In *4th International Conference on Learning Representations, ICLR 2016*, 2016.
- [35] A. Senior, G. Heigold, M. Ranzato, and K. Yang. An empirical study of learning rates in deep neural networks for speech recognition. In *Proceedings of the IEEE International Conference on Acoustics, Speech, and Signal Processing (ICASSP)*, 2013.
- [36] X. Shang, E. Kaufmann, and M. Valko. A simple dynamic bandit algorithm for hyper-parameter tuning. In *Workshop on Automated Machine Learning at International Conference on Machine Learning (AutoML@ICML 2019)*, 2019.
- [37] D. Silver, A. Huang, C. J. Maddison, A. Guez, L. Sifre, G. Van Den Driessche, J. Schrittwieser, I. Antonoglou, V. Panneershelvam, M. Lanctot, et al. Mastering the game of go with deep neural networks and tree search. *Nature*, 529(7587):484–489, 2016.
- [38] R. S. Sutton. Adapting bias by gradient descent: an incremental version of delta-bar-delta. In *Proceedings of the Tenth National Conference on Artificial Intelligence*, pages 171–176. AAAI Press, 1992.
- [39] R. S. Sutton and A. G. Barto. *Reinforcement Learning: An Introduction*. A Bradford Book, Cambridge, MA, USA, 2018. ISBN 0262039249.
- [40] M. E. Taylor and P. Stone. Transfer Learning for Reinforcement Learning Domains: A Survey. *Journal of Machine Learning Research*, 10:1633–1685, 2009.
- [41] T. Tieleman and G. Hinton. Lecture 6.5 - RMSProp: Divide the gradient by a running average of its recent magnitude. Coursera: Neural Networks for Machine Learning, 2012. URL https://www.cs.toronto.edu/~tijmen/csc321/slides/lecture_slides_lec6.pdf.
- [42] H. van Hasselt, A. Guez, and D. Silver. Deep Reinforcement Learning with Double Q-Learning. In *Proceedings of the AAAI conference on artificial intelligence*, 2016.

- [43] O. Vinyals, I. Babuschkin, W. M. Czarnecki, M. Mathieu, A. Dudzik, J. Chung, D. H. Choi, R. Powell, T. Ewalds, P. Georgiev, et al. Grandmaster level in StarCraft ii using multi-agent reinforcement learning. *Nature*, 575(7782): 350–354, 2019.
- [44] P. R. Wurman, S. Barrett, K. Kawamoto, J. MacGlashan, K. Subramanian, T. J. Walsh, R. Capobianco, A. Devlic, F. Eckert, F. Fuchs, et al. Outracing champion Gran Turismo drivers with deep reinforcement learning. *Nature*, 602(7896):223–228, 2022.
- [45] Z. Xu, H. P. van Hasselt, M. Hessel, J. Oh, S. Singh, and D. Silver. Meta-Gradient Reinforcement Learning with an Objective Discovered Online. In *Advances in Neural Information Processing Systems*, volume 33, pages 15254–15264. Curran Associates, Inc., 2020.
- [46] K. You, M. Long, J. Wang, and M. I. Jordan. How does learning rate decay help modern neural networks?, 2019. Preprint, arXiv:1908.01878.
- [47] K. Young, B. Wang, and M. E. Taylor. Metatrace Actor-Critic: Online Step-Size Tuning by Meta-gradient Descent for Reinforcement Learning Control. In *Proceedings of the Twenty-Eighth International Joint Conference on Artificial Intelligence, IJCAI-19*, pages 4185–4191, 2019. doi: 10.24963/ijcai.2019/581.

A Related Work

This section presents works closely related to ours. We first introduce approaches that use MAB for hyperparameter selection and later other methods that aim to adapt the learning rate over the training process.

Multi-armed bandit for (hyper)parameter selection. Deep RL is known to be overly optimistic in the face of uncertainty [28], and many works have addressed this issue by proposing conservative policy updates [42, 14, 2]. However, when the agent can interact with the environment, this optimism might encourage exploration, potentially leading to the discovery of higher returns. Building on this idea, Moskovitz et al. [27] proposes *Tactical Optimism and Pessimism* (TOP), an approach that uses an adversarial MAB algorithm to trade-off between pessimistic and optimistic policy updates based on the agent’s performance over the learning process. Although our work shares similarities with TOP, such as employing an adversarial bandit algorithm and using performance improvement as feedback, there are key differences. First, TOP is closely tied to actor-critic methods, making it unclear how it could be extended to other RL paradigms. Moreover, it also introduces an exploration strategy which depends on epistemic uncertainty (captured through ensembles) and aleatoric uncertainty (estimated using a distributional RL algorithm). Second, TOP trades-off between optimism and pessimism by adding new variables (arms), which are not inherently tied to the learning process and also require tuning. In contrast, LRRL offers an algorithm-agnostic solution by directly optimizing the learning rate, a core hyperparameter in all SGD-based methods, making it simpler and more broadly applicable. Also close to our work, Liu et al. [24] propose Adam with Bandit Sampling (ADAMBS), which employs the Exp3 algorithm to enhance sample efficiency by incorporating importance sampling within the Adam optimizer. ADAMBS prioritizes informative samples by keeping a probability distribution over all samples, although the feedback is provided by the gradient computed over a mini-batch, unlike previous works in RL that are capable of assigning per-sample importance by using their computed TD-error (see 34).

In order to select the learning rate for stochastic gradient MCMC, Coullon et al. [10] employ an algorithm based on Successive Halving [17, 16], a MAB strategy that promotes promising arms and prunes suboptimal ones over time. In the context of hyperparameter optimization, Successive Halving has also been used in combination with infinite-arm bandits to select hyperparameters for supervised learning [22, 36]. A key difference between these approaches to hyperparameter optimization for supervised learning and our work is that we focus on selecting the best learning rate on the fly from a predefined set, rather than performing an extensive and computationally expensive search over the hyperparameter space. Close to our work, Parker-Holder et al. [29] propose population-based training which employs a Gaussian Process (see details in 31) with a time-varying kernel to represent the upper confidence bound in a bandit setting. The idea is to have many instances of agents learning a task in parallel with different hyperparameters, replacing those that are underperforming within a single run.

Learning rate adapters/schedulers. Optimizers such as RMSProp [41] have an adaptive mechanism to update a set of parameters θ by normalizing past gradients, while Adam [18] also incorporates momentum to smooth gradient steps. However, despite their widespread adoption, these algorithms have inherent limitations in non-stationary environments since they do not adapt to changes in the objective function over time (see 13). Increment-Delta-Bar-Delta (IDBD), introduced by Sutton [38], has an adaptive mechanism based on the loss to adjust the learning rate η_i for each sample x_i for linear regression and has been extended to settings including RL [47]. Learning rate schedulers with time decay [35, 46] are coupled with optimizers, assuming gradual convergence to a good solution, but often require task-specific manual tuning. A meta-gradient RL method is proposed in Xu et al. [45], composed of a two-level optimization process: one that uses the agent’s objective and the other to learn meta-parameters of the objective function. Our work differs from these methods by employing a MAB approach to dynamically select the learning rate over the training process, specifically targeting RL settings.

B Supplementary Experiments

B.1 Baseline Evaluation with Varying Learning Rates

To establish a baseline to compare learning without our approach LRRL, we run individual arm values as baseline learning rate using the Adam optimizer. The results presented in Figure 7 align with common expectations by showing that higher learning rates fail to learn for most environments while lower ones can lead to worse jumpstart performance and slow convergence.

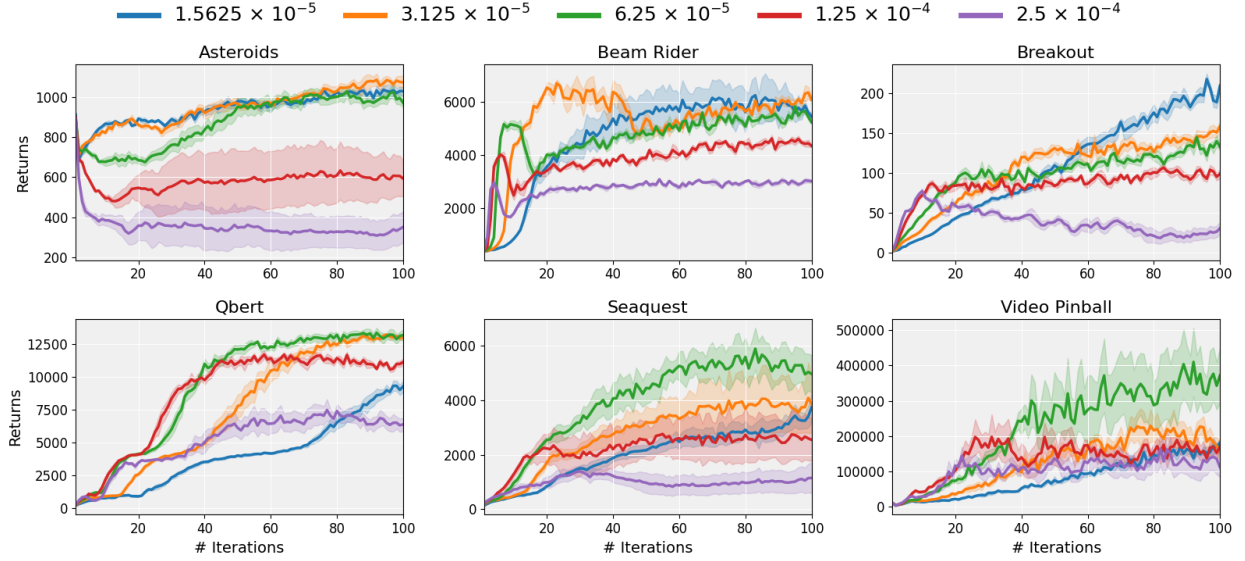


Figure 7: DQN performance using the Adam optimizer with varying learning rates across 6 Atari games. Shaded region represents one-half standard deviation. The results show that the best performing learning rate varies across games.

B.2 A Comparison between Multi-Armed Bandits Algorithms

Adversarial MAB algorithms are designed for environments where the reward distribution changes over time. In contrast, stochastic MAB algorithms assume that rewards are drawn from fixed but unknown probability distributions. To validate our choice and address our method’s robustness, we compare Exp3 with the stochastic MAB algorithm MOSS (Minimax Optimal Strategy in the Stochastic case) [5]. MOSS trades off exploration and exploitation by pulling the arm k with highest upper confidence bound given by:

$$B_k(n) = \hat{\mu}_k(n) + \rho \sqrt{\frac{\max\left(\log \frac{n}{Kn_k(n)}, 0\right)}{n_k(n)}}$$

where $\hat{\mu}_k(n)$ is the empirical average reward for arm k and $n_k(n)$ is the number of times it has been pulled up to round n .

In Figure 8, we use different bandit step-sizes α for Exp3 and parameter ρ , which balances exploration and exploitation in MOSS. Additionally, the bandit feedback used in MOSS is the average cumulative reward $\frac{R}{C}$. The results indicate that while Exp3 performs better overall, MOSS can still achieve competitive results depending on the amount of exploration, demonstrating the robustness of our approach regarding the MAB algorithm employed.

B.3 Dealing with Noise and Lack of Feedback

LRRL relies entirely on performance improvements to update the arm probabilities. However, some RL environments can be highly stochastic, with sparse or delayed rewards, which increases the difficulty of learning tasks and, consequently, the ability of LRRL to make optimal choices. To mitigate this limitation, we introduce the variable κ in Algorithm 1, which determines the number of interactions to observe before making a decision.

When setting κ , two factors should be considered:

- **The network’s update rate:** Selecting new learning rates more frequently than updating the model leads to inaccurate feedback for the bandit mechanism since no model update might occur after pulling some arm.
- **The number of environment steps:** In some tasks, positive or negative outcomes of a sequence of actions are only perceived at the end of an episode, and capturing sufficient information about the agent performance is essential to updating the arms’ probabilities.

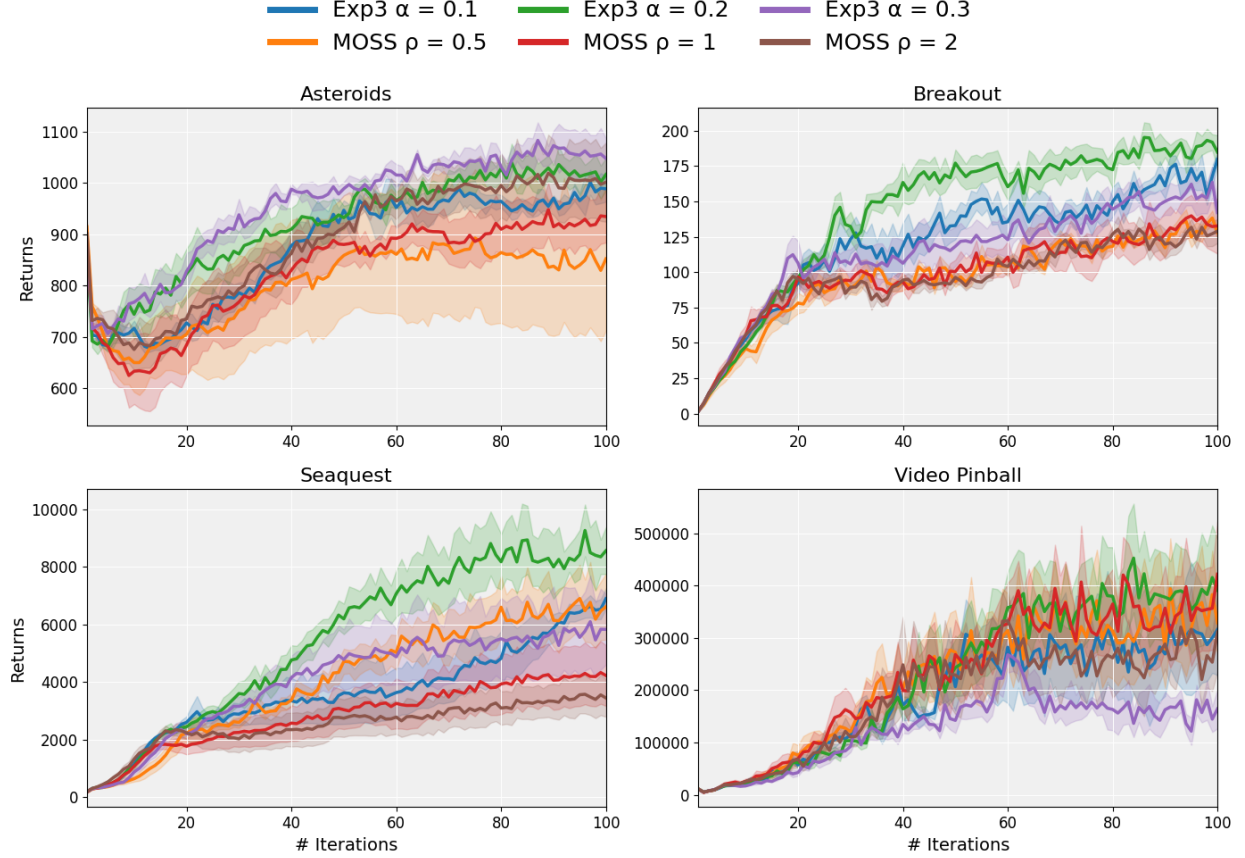


Figure 8: A comparison between adversarial (Exp3) and stochastic (MOSS) MAB algorithms. Shaded region represents one-half standard deviation. The results show that Exp3 performs better overall.

In the experiments presented in this work, we set $\kappa = 1$ episode, allowing the observation of a complete episode before updating the arms' probabilities. To explore the impact of this parameter further, we conduct an ablation study using different κ values to evaluate potential performance improvements when combined with the schedulers shown in Figure 3. As suggested by Figure 9, the choice of κ is task-dependent: while some tasks benefit from more reactive learning rate updates, others show marginal improvements with increased observation counts. Ultimately, setting $\kappa = 1$ seems relatively robust for Atari games, although higher values could slightly increase the performance in some tasks.

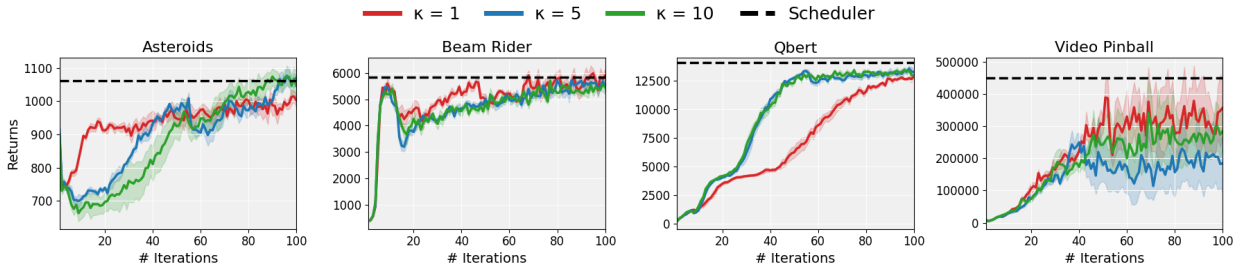


Figure 9: Results of the ablation study evaluating the impact of varying κ with LRRL using schedulers. The dashed black line represents the max average return achieved by the best performing scheduler.

B.4 Supplementary Results using SGD

In Section 4.5, we tested the SGD optimizer in 6 non-convex loss landscapes show in Figure 10. These functions were selected since they represent common benchmarks in optimization, each one offering different challenges due to their distinct shapes. By using SGD on these landscapes, we minimize the influence of confounding factors, such as the high stochasticity inherent in some RL tasks and the complexity of more robust optimizers like Adam.

Figure 11 presents the normalized loss and the arms selected at each optimization step. The results demonstrate LRRL’s dynamic adaptation mechanism, either converging to the most effective learning rate or combining them to achieve superior outcomes.

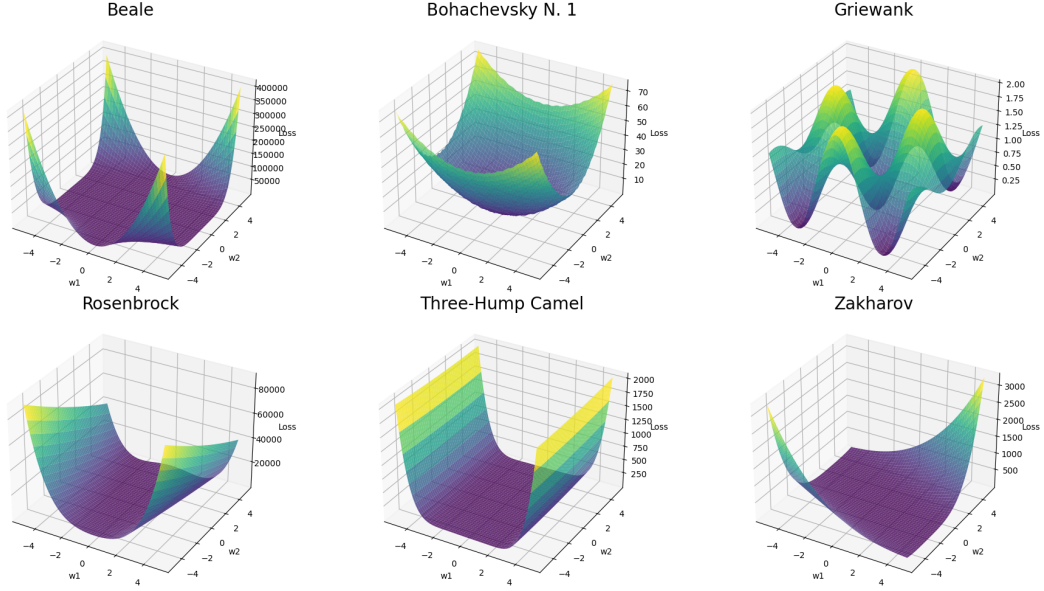


Figure 10: The 6 stationary non-convex loss landscapes used to assess LRRL with SGD optimizer.

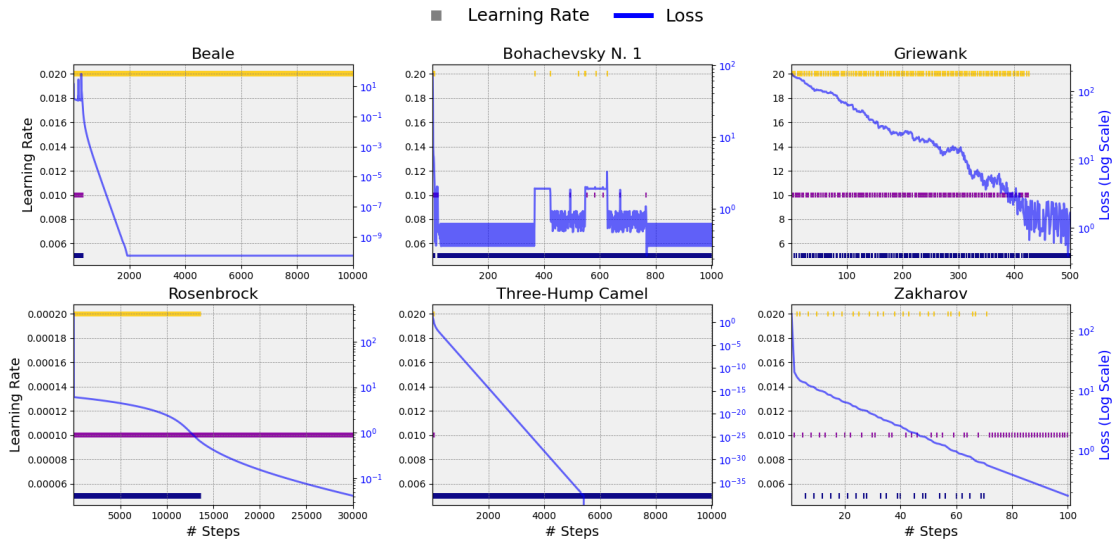


Figure 11: Learning rates and logarithmic scale of losses over the gradient steps using LRRL with SGD optimizer.

C Evaluation Metrics

In this section, we describe the evaluation metrics that can be used to evaluate the agent’s performance as it interacts with an environment. Based on Dopamine, we use the evaluation step-size “iterations”, defined as a predetermined number of episodes. Figure 12 illustrates the evaluation metrics used in this work, as defined in Taylor and Stone [40]:

- **Max average return:** The highest average return obtained by an algorithm throughout the learning process. It is calculated by averaging the outcomes across multiple individual runs.
- **Final performance:** The performance of an algorithm after a predefined number of interactions. While two algorithms may reach the same final performance, they might require different amounts of data to do so. This metric captures the efficiency of an algorithm in reaching a certain level of performance within a limited number of interactions. In Figure 12, the final performance overlaps with the max average return, represented by the black dashed line.
- **Jumpstart performance:** The performance at the initial stages of training, starting from a policy with randomized parameters θ . In Figure 12, Algorithm A exhibits better jumpstart performance but ultimately achieves lower final performance than Algorithm B. A lower jumpstart performance can result from factors such as a lower learning rate, although this work demonstrates that this does not necessarily lead to worse final performance.

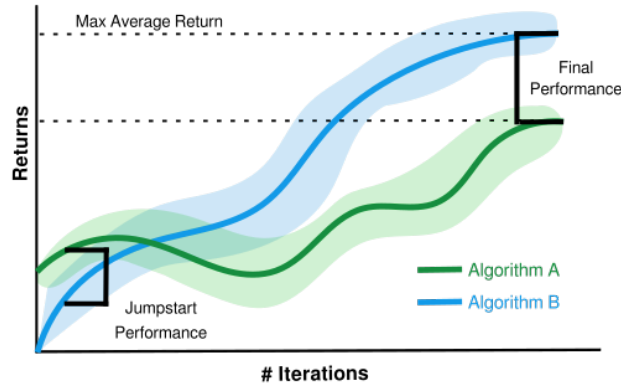


Figure 12: Performance curves of two RL algorithms (adapted from 40).

D Implementation Details

In the following, we list the set of arms, optimizer and the bandit step-size used in each experiment.

Section 4.1 – Comparing LRRL with Standard Learning.

- Optimizer: Adam
- Bandit step-size: $\alpha = 0.2$
- Considered sets of learning rates:

$$\mathcal{K}(5) = \{1.5625 \times 10^{-5}, 3.125 \times 10^{-5}, 6.25 \times 10^{-5}, 1.25 \times 10^{-4}, 2.5 \times 10^{-4}\}$$

$$\mathcal{K}_{\text{lowest}}(3) = \{1.5625 \times 10^{-5}, 3.125 \times 10^{-5}, 6.25 \times 10^{-5}\}$$

$$\mathcal{K}_{\text{middle}}(3) = \{3.125 \times 10^{-5}, 6.25 \times 10^{-5}, 1.25 \times 10^{-4}\}$$

$$\mathcal{K}_{\text{highest}}(3) = \{6.25 \times 10^{-5}, 1.25 \times 10^{-4}, 2.5 \times 10^{-4}\}$$

$$\mathcal{K}_{\text{sparse}}(3) = \{1.5625 \times 10^{-5}, 6.25 \times 10^{-5}, 2.5 \times 10^{-4}\}$$

Section 4.2 – Combining and Comparing Schedulers with LRRL.

- Optimizer: Adam
- Bandit step-size: $\alpha = 0.2$
- Initial learning rate of schedulers: $\eta_0 = 6.25 \times 10^{-5}$

Section 4.3– Comparing RMSProp and Adam Optimizers

- Optimizer: RMSProp for DQN baselines
- Bandit step-size: $\alpha = 0.2$
- LRR-DQN set of learning rates: $\mathcal{K} = \{1.5625 \times 10^{-5}, 3.125 \times 10^{-5}, 6.25 \times 10^{-5}\}$

Section 4.4– LRRL with a Distributional RL Algorithm.

- Optimizer: Adam
- Bandit step-size: $\alpha = 0.2$
- LRRL-IQN set of learning rates: $\mathcal{K} = \{2.5 \times 10^{-5}, 5 \times 10^{-5}, 1 \times 10^{-4}\}$

Section B.2 – A Comparison between Multi-Armed Bandit Algorithms.

- Optimizer: Adam
- MOSS/Exp3 set of learning rates: $\mathcal{K} = \{3.125 \times 10^{-5}, 6.25 \times 10^{-5}, 1.25 \times 10^{-4}\}$

Hyperparameters of the optimizers and deep RL algorithms. For reproducibility, the list of hyperparameters of the optimizers and deep RL algorithms used for our experiments is provided in Table 1. The optimizers from the Optax library [12] are employed alongside the JAX [8] implementation of the DQN [25, 26] and IQN [11] algorithms, as provided by the Dopamine framework [9].

DQN and IQN hyperparameters	Value
Sticky actions	True
Sticky actions probability	0.25
Discount factor (γ)	0.99
Frames stacked	4
Mini-batch size (\mathcal{B})	32
Replay memory start size	20 000
Learning network update rate (λ)	4 steps
Minimum environment steps (κ)	1 episode
Target network update rate (τ)	8000 steps
Initial exploration (ϵ)	1
Exploration decay rate	0.01
Exploration decay period (steps)	250 000
Environment steps per iteration (steps)	250 000
Reward clipping	[-1, 1]
Network neurons per layer	32, 64, 64
Hardware (GPU)	V100
Adam hyperparameters	
β_1 decay	0.9
β_2 decay	0.999
Eps (DQN)	1.5×10^{-4}
Eps (IQN)	3.125×10^{-4}
RMSProp hyperparameters (DQN)	
Decay	0.9
Momentum (if <i>True</i>)	0.999
Centered	False
Eps	1.5×10^{-4}

Table 1: Hyperparameters used in the experiments.